Response Spectrum Solutions for Blast Loading

Nelson Lam[1], Priyan Mendis[2], Tuan Ngo[3]
Advanced Protective Technology for Engineering Structures (APTES) Research Group
Department of Civil & Environmental Engineering,
The University of Melbourne
Parkville 3010, Victoria, Australia

ABSTRACT

Existing knowledge on the modelling of blast pressure have been further developed in this paper for engineering applications. Parametric studies involving time-history analyses of simple cantilevered wall models have been undertaken based on pre-defined pressure functions to study basic trends. The "corner period" of the velocity response spectrum was found to be the key controlling parameter in response behaviour modelling of the walls. An important contribution from this study is the identification of the direct relationship between the corner period and the "clearing time" for the blast. A simple and yet realistic capacity spectrum model has been developed for the design and assessment of cantilevered walls for its performance under blast loads. The practicality of the proposed model has been demonstrated herein by a worked example.

KEYWORDS

Blast pressure, explosion, response spectrum, cantilevered walls

1 Introduction

Research has been undertaken over the past half a century on the modelling of blast pressure on objects and structures [Brode,1955; Henrych,1979; Kingery,1984; Smith,1994]. The recommended expressions for the blast generated maximum (peak) static over-pressure enable predictions to be made in the open field for any given stand-off distance and blast load expressed in terms of TNT equivalence. The reflected over-pressure resulted from interaction of the blast wave with a stationary target surface has also been modelled (Smith,1994). It will be shown in this paper that the impact of the blast wave on a structure depends not only on the peak blast pressure but also the duration in which the pressure is sustained. A more detailed description of the variation of the blast pressure with time is given in Section 2. New correlations not published previously will be presented to facilitate the determination of parameters associated with the blast pressure function (eg. quadratic expression of the “b” parameter in Eq.5).

In this study, rectangular blast walls were subject to linear elastic dynamic analyses based on the blast pressure function defined in Section 2. Each wall was treated as a single-degree-of-freedom substitute structure in the analyses. Refer Section 3 for a description of the analysis results.

The computed response behaviour will be presented in the form of acceleration and displacement time-histories along with response spectra presented in the different formats including the *ADRS* diagram (which is also known as the capacity spectrum). Simplified response spectrum models forming the key contributions of this paper will be proposed for facilitating engineering applications. This paper concludes with an illustration of the proposed procedure by a worked example in Section 7.

2 Modelled Blast Pressure

Expressions for the maximum (or peak) static over-pressure (Ps_{max}) developed in a blast have been presented in the literature to model free-field conditions in which dynamic interactions of the wavefront with objects obstructing the blast wave path is small enough to be neglected. Ps_{max} have typically been correlated with the scaled distance parameter (Z) which is defined by Eq.1

$$Z = \frac{R}{W^{1/3}} \tag{1}$$

where R is standoff distance in metres

and W is the charge weight of the blast in kg based on TNT equivalence

Brode [1955] developed the correlation between Ps_{max} and Z based on numerical modelling (see Figure 1). This correlation was subsequently reviewed by Smith [1994] who compared Brode's model with results obtained from more recent experimental studies. The comparison shows excellent consistency between the models in the far-field whilst Brode's model tends to be conservative in the near field (Z<<1). The model is considered valid within the range of z=0.2-2. The over-pressure varies by about three orders of magnitude within this range of Z (1-1000 bar). An amplification factor of 1.8 has been applied to account for the effects of waves reflecting from the ground surface in the common “hemispherical” blast scenarios.

Previous investigations have also identified a significant negative (suction) pressure which is developed shortly after the subsidence of the positive (compressive) over-pressure. The absolute value of this "minimum" pressure (denoted Ps_{min}) is presented in Figure 1 along with the maximum (positive) over-pressure.

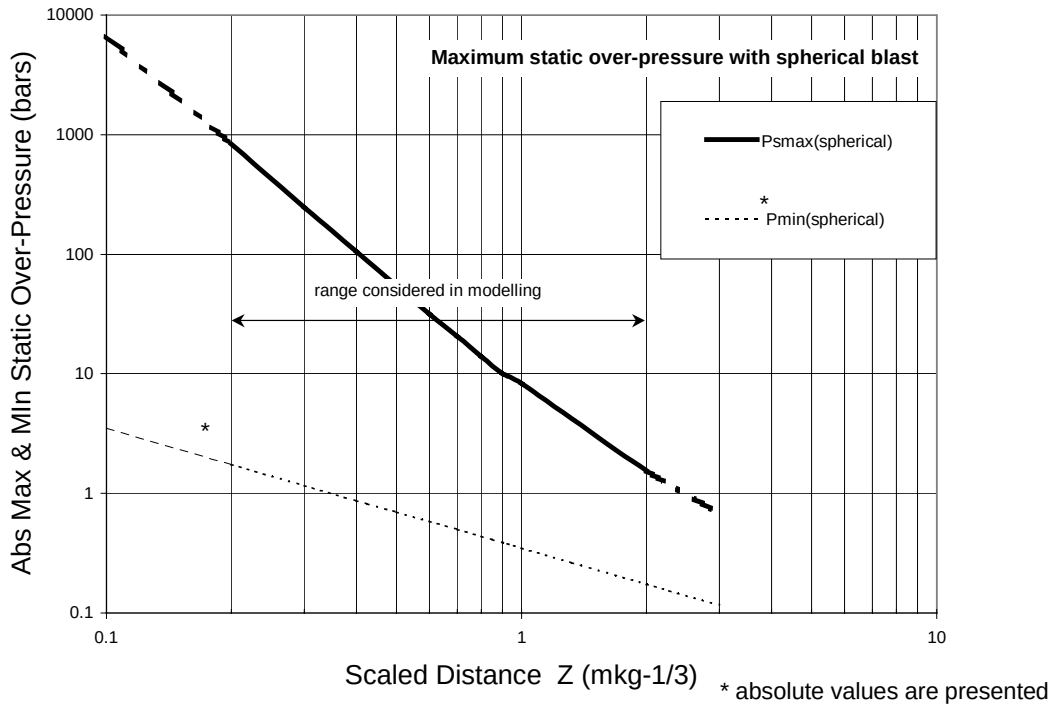

Figure 1 Maximum and Minimum Static Over-pressure with Spherical Blast

The well known Friedlander wave equation (Eq.2) defines the rise and fall of the static over-pressure (***Ps***) with time as shown by the example presented in Figure 2 (for Z=1).

$$Ps(t) = 1.8 Ps_{max}\left(1 - \frac{t}{T_s}\right) exp^{\frac{-bt}{T_s}} \qquad (2)$$

where the "1.8" factor accounts for the effects of a hemispherical blast

b is the parameter controlling the rate of wave amplitude decay

and T_s is the parameter characterising the duration of the blast pulse (see Figure 2).

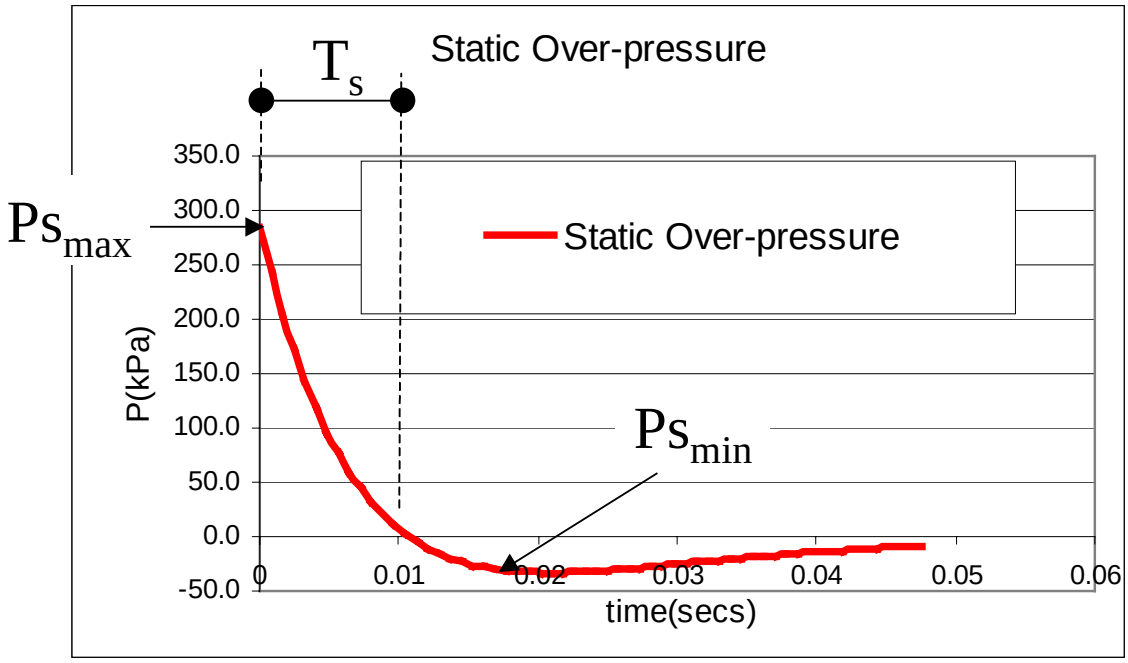

Figure 2: Friedlander's Blast Pressure Function (Z=2,W=125kg,R=10m)

T_s has been correlated with the standoff distance (***R***) by Smith (1994). This correlation can be approximated conservatively by Eq.3 which defines a linear relationship between T_s and ***R*** in a log-log format with ***Z*** being held constant.

$$\log_{10}\left(\frac{T_s}{W^{1/3}}\right) \approx -2.75 + 0.27 \log_{10}\left(\frac{R}{W^{1/3}}\right) \qquad (3)$$

With W=1000kg and R=10m for example, T_s is estimated at approximately 0.018sec (see Figure 2).

The ratio of the absolute minimum and maximum pressure (Ps_{min}/Ps_{max}) predicted by the Brode's model (Figure 1) is not constant but varies significantly with scaled distance ***Z***. The relative significance of the negative pressure (represented by this ratio) is shown to increase with increasing values of ***Z*** (see Figure 3).

The "***b***" parameter in Eq.2 can be related to the ratio (Ps_{min}/Ps_{max}). Mathematical manipulations of Eq.2 by the authors resulted in Eq.4 (see also Figure 4).

$$ln\left(b\left|\frac{Ps_{min}}{Ps_{max}}\right|\right)+b+1=0 \qquad (4)$$

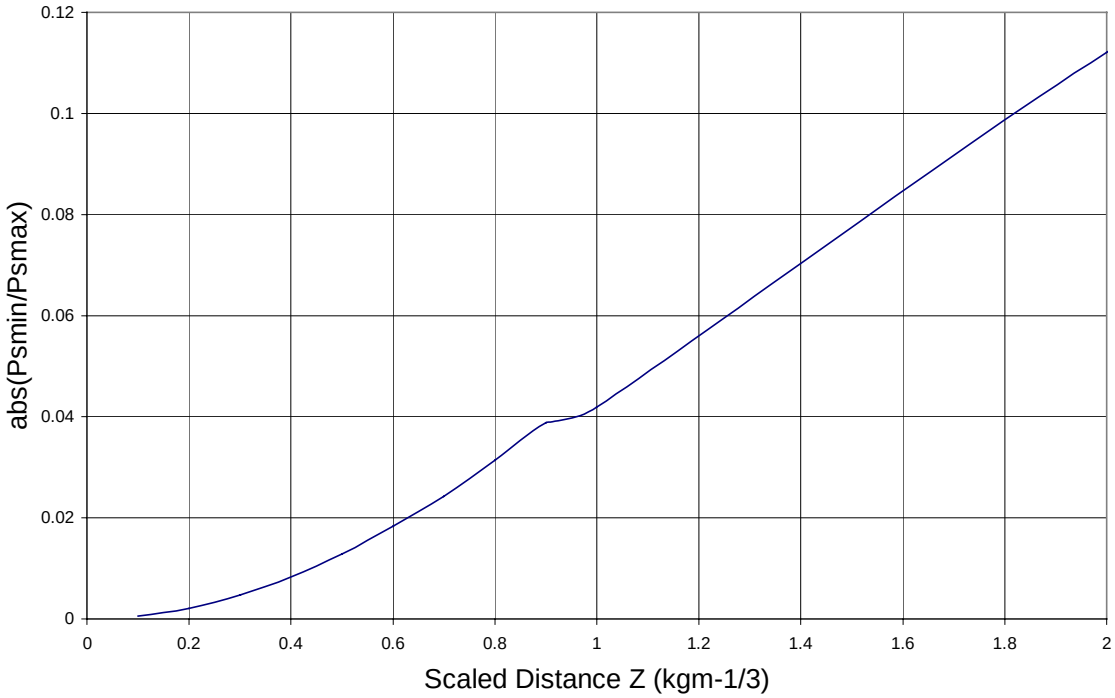

Figure 3: Relative significance of positive and negative pressure

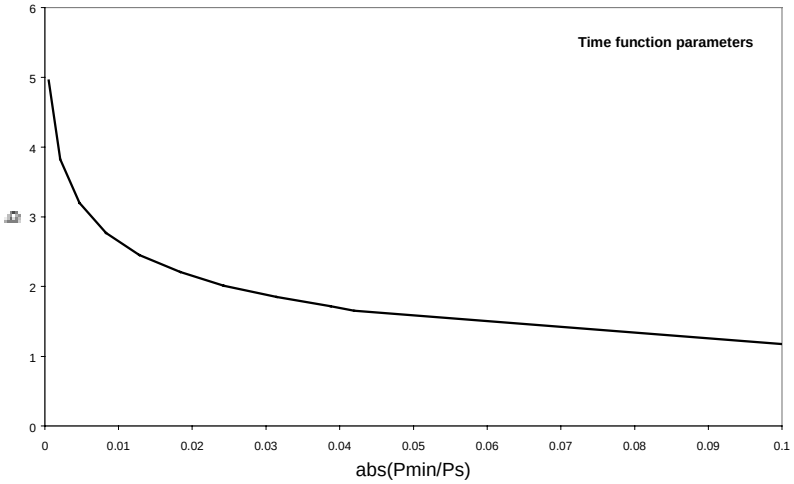

Figure 4: Correlation of the *b* parameter with abs(Ps_{min}/Ps_{max})

The relationships presented in Figures 3 & 4 have been combined by the authors to produce Figure 5 which describes the variation of the "***b***" parameter with scaled distance ***Z***. The explicit correlation between ***b*** and ***Z*** as shown in Figure 5 shall facilitate the computation of the

pressure function for any given blast scenario for the future. The quadratic curve-fit (with R^2=0.96) is accordingly given by Eq.5.

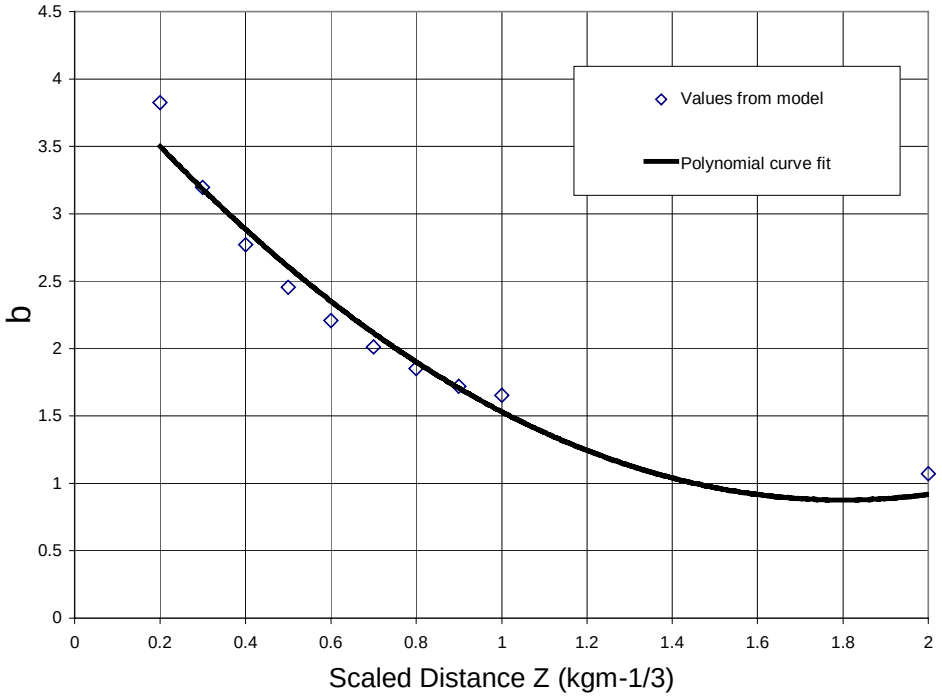

Figure 5: Correlation of the "b" parameter with Z

$$\boldsymbol{b} = \boldsymbol{Z}^2 - 3.7\boldsymbol{Z} + 4.2 \tag{5}$$

The reflected over-pressure (Pr) arising from the interaction of the blast waves with a flat-surface (obstructing the passage of the wavefront) has been modelled by Smith (1994) and is approximated by Eq.6 proposed in this paper based on the conservative assumption of zero angle of incidence (see also Figure 6).

$$\boldsymbol{Pr_{max}} = \boldsymbol{Cr}.\boldsymbol{Ps_{max}} \quad \textit{where}$$
$$\boldsymbol{Cr} = 3\left(\sqrt[4]{\boldsymbol{Ps_{max}}}\right) \tag{6}$$

where $\boldsymbol{P_{Smax}}$ is in units of bars and $\boldsymbol{Cr}$ is the coefficient for the reflected over-pressure.

It has been shown in the model presented by Smith (1994) that the reflected over-pressure is not sensitive to the angle of incidence up to 40deg. (for $\boldsymbol{Ps_{max}}$ less than 50bars). The reflected over-pressure drops off abruptly as the critical angle of 40deg is reached. In this study, a conservative zero angle of incidence has been assumed in the calculation of the reflected over-pressure (see Section 3 for further details). The reflected over-pressure will need to be superposed on the static over-pressure in modelling the total impact of the blast wave on the flat surface as shown in Figure 7. An important parameter in the reflected over-pressure is the "clearing time" $\boldsymbol{T}$'' which defines the time taken for the reflected over-pressure to decay completely and can be estimated by Eq.7a (Smith, 1994).

$$\boldsymbol{T}' = \frac{3\boldsymbol{S}}{\boldsymbol{U}} \tag{7a}$$

where $\boldsymbol{S}$ = minimum dimension on the frontal surface of the blast
$\boldsymbol{U}$ = blast front velocity which is given by Eq.7b.

$$U = \sqrt{\frac{6Ps_{\max} + 7P_o}{7P_o}}.a_o \qquad (7b)$$

where Ps_{max} has been defined above (and can be obtained from Figure 1), P_o is the ambient pressure (*~1bar* or *101kPa* typically) and a_o is the speed of sound (*335m/sec*).

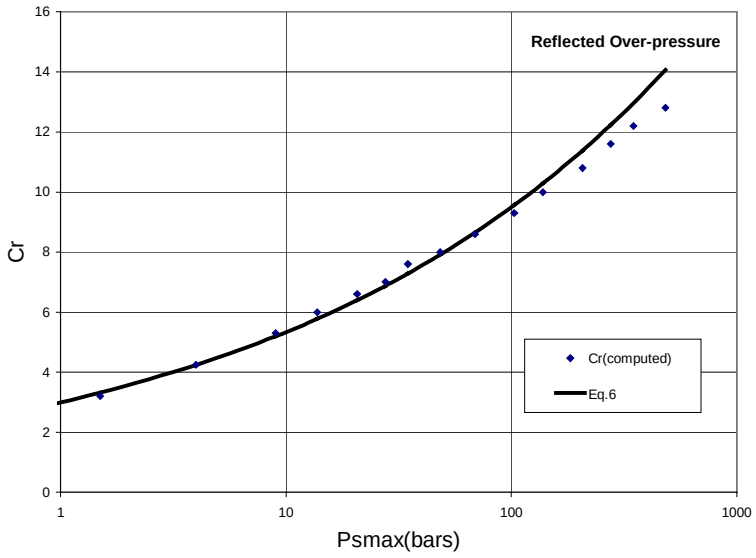

Figure 6: Coefficient for Reflected Over-Pressure

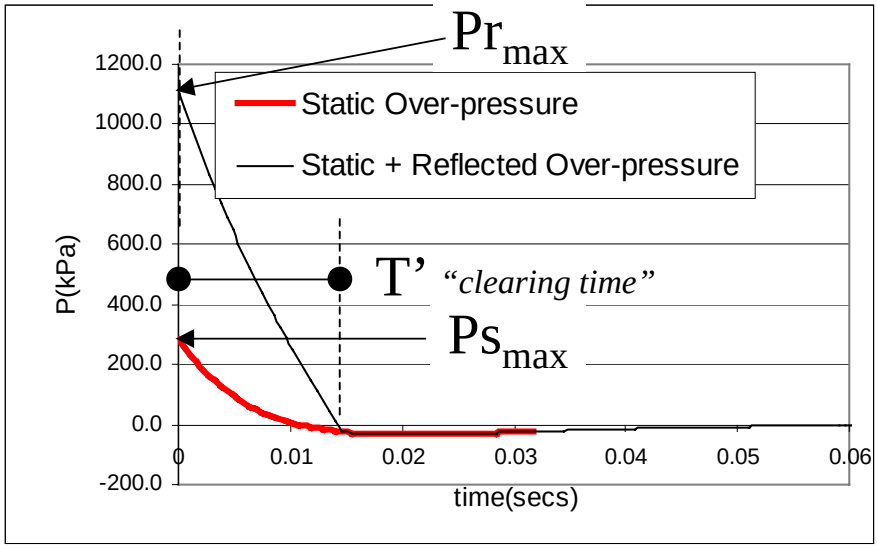

Figure 7: Static and Reflected Over-pressures (Z=2,W=125kg,R=10m)

2.1 Single-degree-of-freedom Responses

In this study, rectangular wall panels of 3m high by 1m wide were subject to linear elastic dynamic analyses based on pre-defined blast pressure functions defined in Section 2. Uniform static and reflected over-pressure (P_s+P_r) based on a minimum stand-off distance of R and zero angle of incidence was applied on the wall as shown in Figure 8. The total blast load $F(t)$ is given by Eq.8

$$F(t) = (P_s + P_r)(1)(H) = 3(P_s + P_r) \tag{8}$$

Eq.8 may be taken as a conservative approximation to the total blast load in view of the decrease in the blast pressure with increasing offset from the wall centerline as shown in Figure 8.

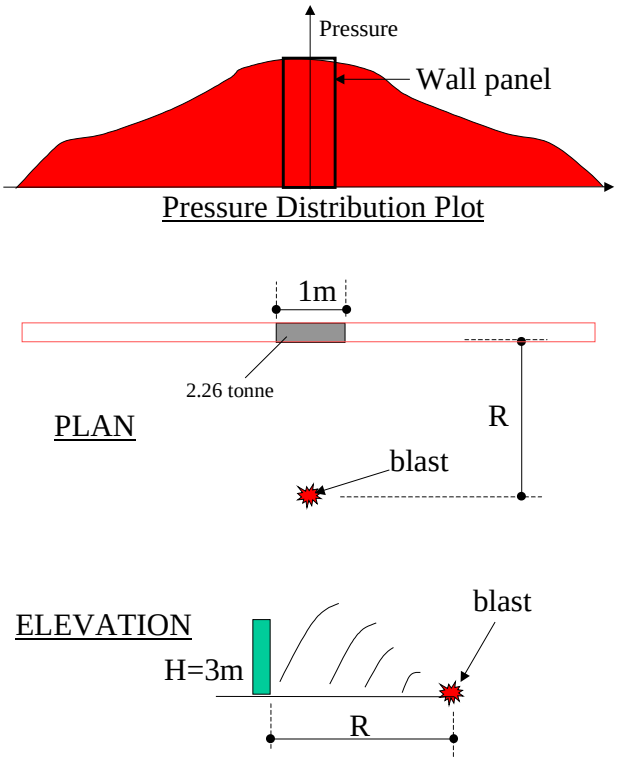

Figure 8: Model Blast Wall

The response acceleration time-histories were calculated by the substitute-structure modelling technique which has been well publicized in the earthquake engineering literature (eg. ATC40[1997]). By substitute-structure modeling, the cantilevered wall panel is treated as a single-degree-of-freedom lumped mass system with effective natural period T_e defined by Eq.9.

$$T_e = 2\pi\sqrt{\frac{M_e}{K_e}} \tag{9}$$

where M_e is the wall effective mass which is approximately ¾ of the total mass of the cantilevered wall panel and K_e is the effective stiffness which can be taken as the total base shear divided by the displacement at two-thirds up the wall height (when the wall is subject to a quasi-static load simulating the blast pressure).

Preliminary analyses were undertaken for a blast load generated by ***W***=125kg of TNT equivalence at a standoff distance of ***R***=10m (ie ***Z***=*2*). The maximum total pressure imposed by the blast was approximately 1100kPa (see Figure 7). Two walls were subject to this blast loading. The total mass on each wall was 2.26 tonnes so that the notional peak acceleration (***PA***) imposed by the blast on the wall (ie total blast load/total wall mass) is equal to 150g's. In theory, a "perfectly rigid" wall with "zero" natural period would experience this notional ***PA***. In comparison, the two walls analysed in this study possessed a natural period of 0.05sec and 0.2sec respectively. Their computed maximum response accelerations differed by a factor of four (being 100g's and 25g's respectively) and both were much less than the notional ***PA*** value of 150g's.

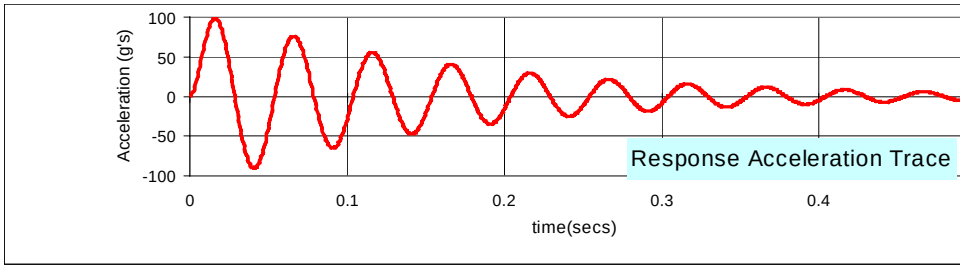

(a)Natural Period=0.05sec

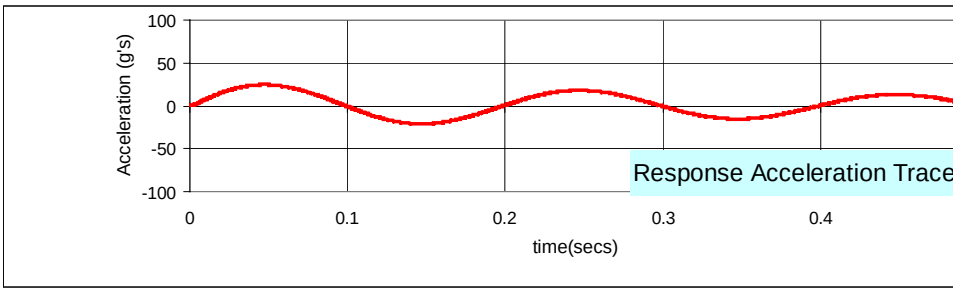

(b)Natural Period=0.2sec

Figure 9: Wall Response Acceleration Time-Histories (*W*=125kg,R=10m)

The uncertainties associated with the wall dynamic response behaviour as shown in the illustrated examples suggest the need for a response spectrum approach in the modelling. In the rest of this paper, response spectra of different formats will be used in modelling the seemingly complex behaviour trends associated with the blast loading.

3 Representation by Acceleration Response Spectra

The response behaviour of the wall panel can be represented by the acceleration response spectrum as shown in Figure 10a for the blast load generated by a charge mass of ***W***=125kg TNT equivalence and at a standoff distance of ***R***=10m. The response spectrum is in the form of a hyperbola and with the "asymptote" occurring at a natural period which is much lower than 0.05sec. Consequently, the maximum response acceleration shown by the time-history of Figure 9a (based on T=0.05sec) is much lower than the notional ***PA*** limit. The effects of the alternative blast scenario of ***W***=125kg at ***R***=20m is represented by a different, but similar looking, response spectrum as shown in Figure 10b. Response spectra for the two blast scenarios are different despite that both scenarios have the same scaled distance (***Z***) and consequently same peak over-pressure (Ps_{max}). For example, response spectral accelerations of 24g's and 28g's respectively are shown at a common natural period of 0.2sec .

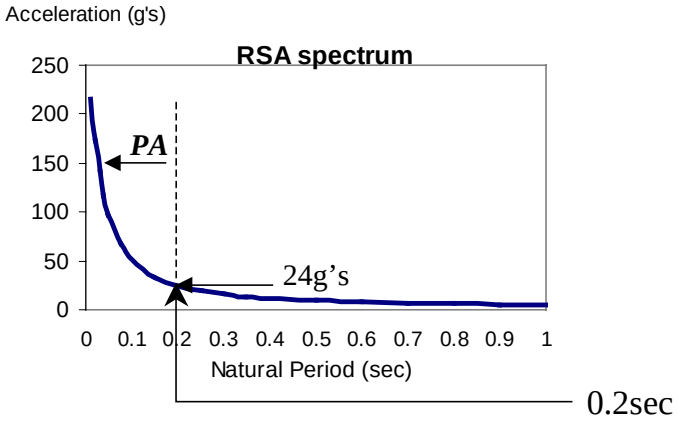

(a) ***W***=125kg,***R***=10m (Z=2)

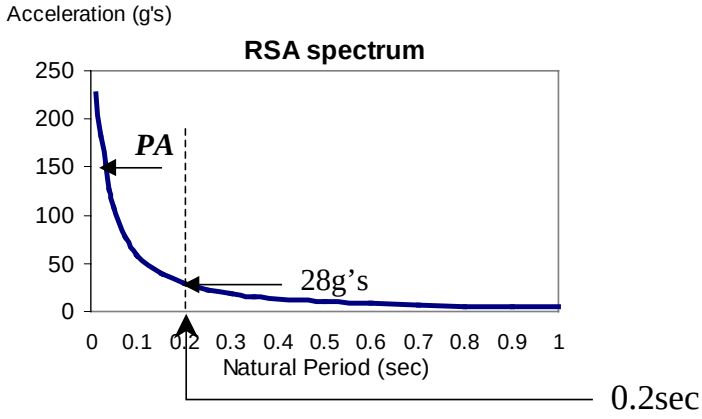

(b) ***W***=1000kg,***R***=20m (Z=2)

Figure 10 Wall Acceleration Response Spectra

It is evident from the above that there are considerable uncertainties in the estimated response spectral acceleration of the building due to the sensitivity of the spectral acceleration to variations in the wall natural period particularly in the low period range. Furthermore, the spectral acceleration varies with the blast scenario even if the notional *PA* has been held constant.

4 Representation by Velocity Response Spectra

The wall response behaviour associated with the blast scenarios defined in Section 4 could be presented in the alternative velocity response spectrum format. The review paper by Chandler *et al* (2001) provides detailed explanations for the use of response spectra in the different formats. Although the illustrations were given in the context of earthquake engineering, they would be equally applicable to representations for blast loading. Importantly, the response spectral velocity (***RSV***) which represents the impulse delivered by the blast converges to a maximum value ($\boldsymbol{RSV}_{max}$) when approaching the high period end of the spectrum as shown in Figure 11a&b for the two blast scenarios presented in Section 4. Both velocity spectra can be represented by a simplified and conservative bi-linear spectrum as defined by Eq.10.

$$\boldsymbol{RSV} = \boldsymbol{PA}.\frac{\boldsymbol{T}}{2\pi} \quad (\text{for } \boldsymbol{T} \le \boldsymbol{T}_1) \tag{10a}$$

$$\boldsymbol{RSV} = \boldsymbol{PA}.\frac{\boldsymbol{T}_1}{2\pi} = \text{RSV}_{\max} \quad (\text{for } \boldsymbol{T} > \boldsymbol{T}_1) \tag{10b}$$

where $\boldsymbol{T_1}$ is the corner period.

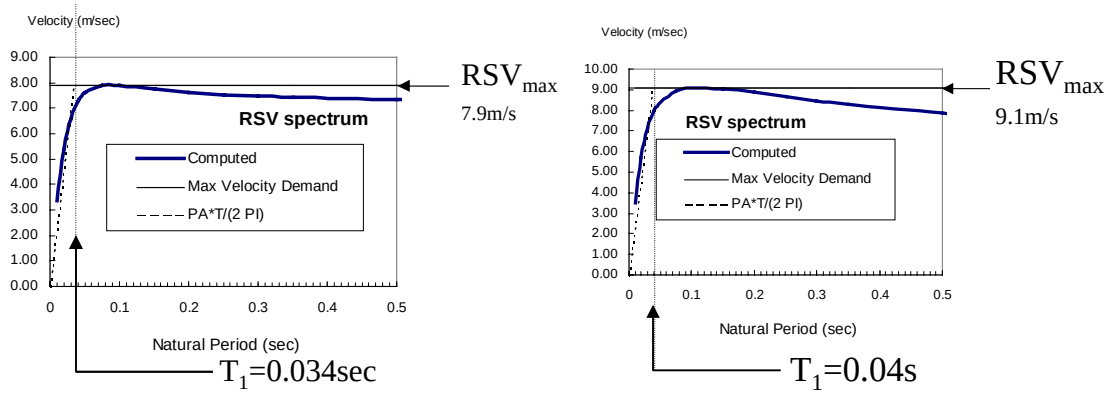

(a) W=125kg, R=10m, Z=2 (b)W=1000kg, R=20m, Z=2

Figure 11: Wall Velocity Response Spectra

It is shown in Figure 11 that the two blast scenarios which produces identical blast pressure (hence identical ***PA***) developed different levels of impulses (represented by $\boldsymbol{RSV_{max}}$). Central to the construction of the bi-linear velocity response spectrum is the corner period $\boldsymbol{T_1}$ which varies with the blast scenario even if the maximum blast pressure has been kept constant**.** For any given value of the blast pressure (and hence ***PA***), the maximum response spectral velocity $\boldsymbol{RSV_{max}}$ increases with increasing value of $\boldsymbol{T_1}$.

The duration of the blast $\boldsymbol{T_s}$ increases with the scaled distance ***Z*** (according to Eq.3), and consequently, $\boldsymbol{T_1}$ increases with Z. Furthermore, $\boldsymbol{T_1}$ would also be dependent on the dimension of the front face exposed to the blast. The least dimension of the front face (denoted as ***S***) controls the "clearing time" (***T'***) of the reflected over-pressure according to Eq.7a (refer Figure 7 for illustration of the reflected over-pressure and clearing time).

The significant effects the clearing time (***T'***), or dimension ***S***, has upon the first corner period ($\boldsymbol{T_1}$) is well demonstrated in Figure12(a) in which the values of T_1 calculated for two different dimension parameters (ie ***S***=1m and ***S***=3m) are correlated. The correlations show that the value of T_1 for ***S***=3m is consistently in the order of two times higher than that for ***S***=1m. Further correlations have been obtained for the corner period ratio ($\boldsymbol{T_1/T'}$) which has the clearing time as the denominator. Correlations for this ratio are well constrained between 2.5 and 3, and averaged at around 2.75 for ***S***=3m as shown in Figure 12(b). This ratio is not so well constrained for ***S***=1m.

A simple expression for the corner period ratio (Eq.11) is proposed herein based on linear interpolation between the average ratios obtained at S=1m and 3m.

$$\frac{\boldsymbol{T}_1}{\boldsymbol{T}'} = 3.25 - 0.25(\boldsymbol{S} - 1) \qquad (\boldsymbol{for}\ \boldsymbol{S} = 1\boldsymbol{m}) \tag{11}$$

Eq.11 enables the corner period (T_1) to be determined and the velocity response spectrum constructed based on the estimated clearing time (T'). The latter is defined as a function of S and other basic blast parameters as defined by Eqs.7a & 7b. It is noted in Figure 12(c)-(d) that Eq.11 is conservative in situations of high intensity blast pressure where the scaled distance is relatively small (Z<0.5).

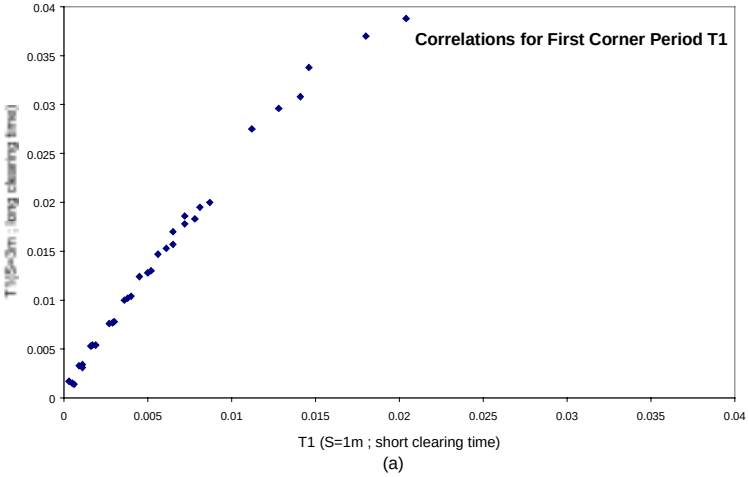

(a)

Figure 12: Behaviour of corner period *T1* and corner period ratio T_1/T'

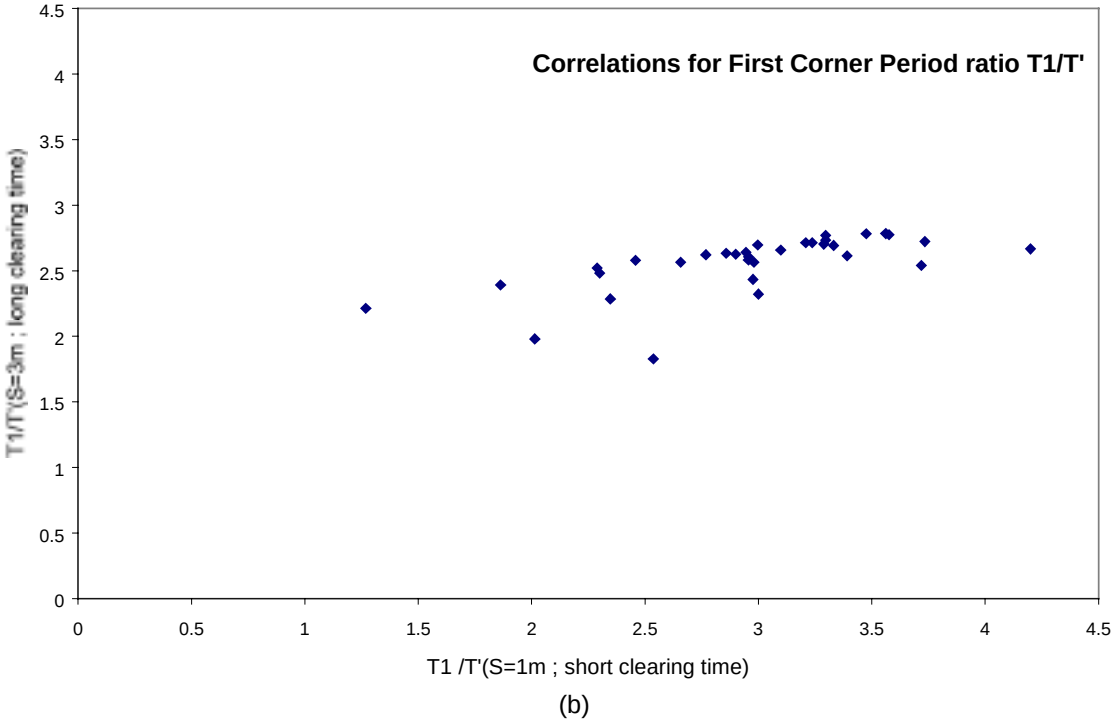

(b)

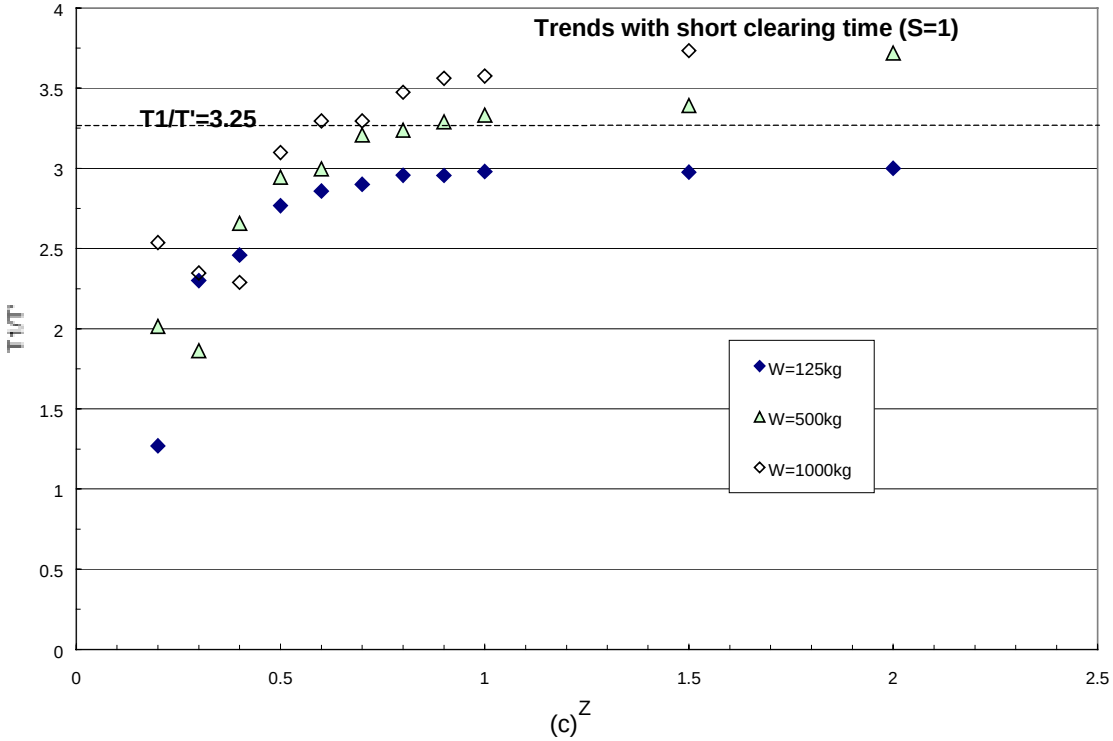

(c)

Figure 12 (continued)

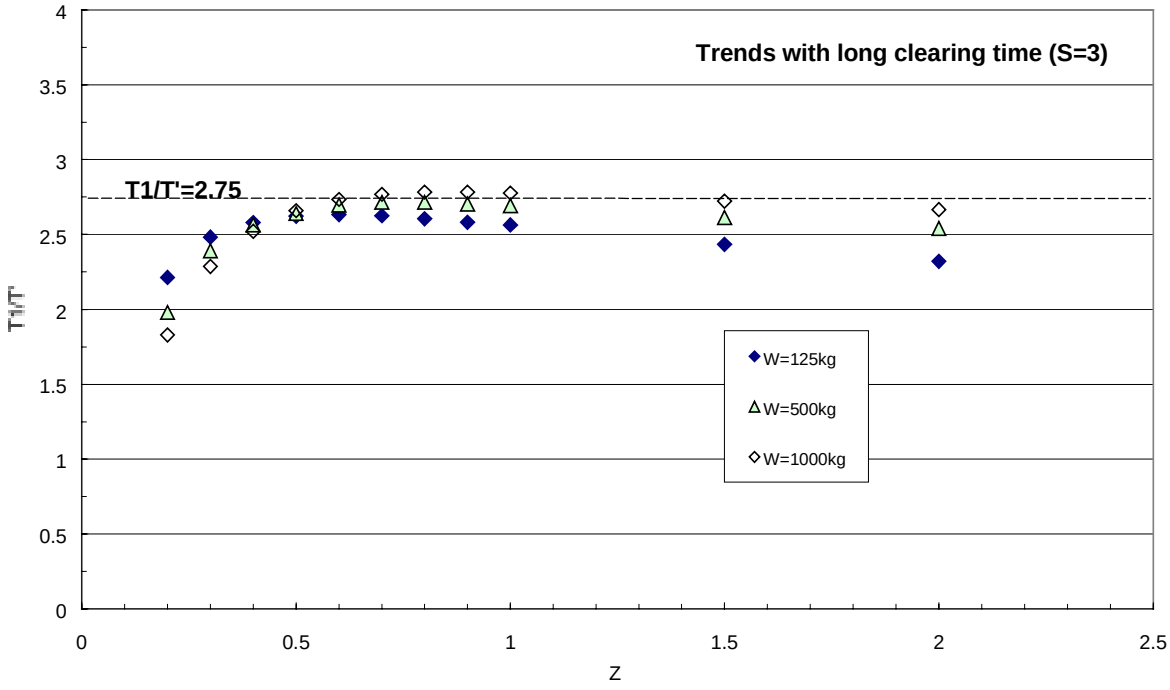

(d)

Figure 12 (continued)

The response spectral velocity (***RSV***) enables the maximum kinetic energy (***KE)*** developed in the wall and resulted from the blast load to be determined (using Eq.12). The wall is deemed to

be capable of withstanding the impact of the blast if the estimated kinetic energy could be absorbed safely by the wall in the form of strain energy.

$$\boldsymbol{KE} = \frac{1}{2}\boldsymbol{M_e}\left(\boldsymbol{RSV}\right)^2 \tag{12}$$

where $\boldsymbol{M_e}$ is the effective mass which is approximately ¾ of the total mass

and $\boldsymbol{RSV}$ is response spectral velocity as read off directly from the velocity spectrum.

5 Representation by Acceleration-Displacement Response Spectrum Diagrams

A direct method to compare "demand" with "capacity" is the acceleration-displacement response spectrum (ADRS) diagram (which is also known as the capacity spectrum) as shown in Figure 13. A review of the inter-relationships between the different response spectrum formats is contained in Lam and Wilson (2004). The expression for the "demand" curve associated with the "flat" part of the velocity spectrum (defined by Eq.10b) can be obtained by equating the maximum kinetic energy with the strain energy of a linear elastic system as shown by Eq.13. The more conservative "simplified" curve identified in Figure 13 is based on this equation.

$$\begin{aligned} &\frac{1}{2}\boldsymbol{M_e}\left(\boldsymbol{RSV}_{\max}\right)^2 = \frac{1}{2}\boldsymbol{F}\Delta \\ &\boldsymbol{a} = \frac{\boldsymbol{F}}{\boldsymbol{M_e}} = \frac{\left(\boldsymbol{RSV}_{\max}\right)^2}{\Delta} \end{aligned} \tag{13}$$

In the capacity spectrum procedure, the capacity curve obtained by the push-over analysis of the wall is intercepted with the demand curve to identify the "performance point". The capacity curve shown in Figure 13 represents a wall with a total mass of 2.26 tonnes (effective mass=1.7tonnes) and an effective natural period of 0.05sec up to a displacement of 0.15m. This is translated into an effective stiffness of approximately 27MN/m which corresponds to an acceleration capacity of about 1600g's/m.

The seismic demand curve is defined by Eq.13 which is a simplified, and conservative representation of the actual demand curve for the blast scenario of W=125kg, R=10m and Z=2 (refer legend in Figure 13). The assumption of 5% damping is also conservative in view of the much higher level of energy absorption associated with the inelastic behaviour of the system. The wall is predicted to displace by about 50-60mm at its center of inertia according to the interception of the demand curve with the capacity curve.

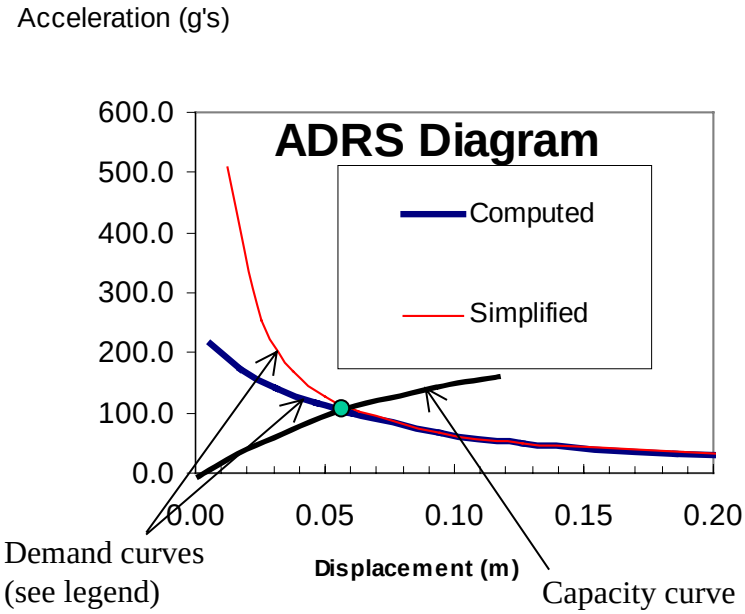

Figure 13: Capacity Spectrum (or ADRS Diagram) for W=125kg,R=10m,Z=2

With the introduction of the response spectrum and ADRS diagrams in the analysis for blast loading, the performance based principles that were initially associated with the design and analysis for earthquake actions have now been broadened to address a much wider range of engineering problems.

6 Summary of procedure and illustration by example

The response spectrum procedure proposed in this paper comprises three key steps as summarized in the following:

*(i) Determination of peak acceleration (**PA**)*

- *calculating scaled distance (**Z**) using Eq.1*
- *calculating maximum static over-pressure $\boldsymbol{Ps_{max}}$ using Figure 1*
- *calculating reflected over-pressure $\boldsymbol{Pr_{max}}$ using Eq.6 and Figure 6*
- *calculating total blast load*
- *calculating peak acceleration **PA** (total blast load/total mass)*

(ii) Determination of first corner period $\boldsymbol{T_1}$ and $\boldsymbol{RSV_{max}}$

- *calculating "clearing time" **T'** using Eq.7*
- *calculating corner period ratio $\boldsymbol{T_1/T'}$ using Eq.11 and Figure 11*
- *calculating $\boldsymbol{RSV_{max}}$ using Eq.10b*

(iii) Determination of displacement and acceleration demand at the "performance point"

- *obtaining demand curve for the ADRS diagram using Eq.13*
- *obtaining capacity curve by push-over analysis*
- *intercepting demand curve with capacity curve to identify performance point*

The above procedure is illustrated herein with a worked example. In the considered blast scenario, a charge weight of 500kg of TNT equivalence is detonated at a minimum standoff distance of 12m from the wall panel as shown in Figure 14. The cantilevered wall panel has a total mass of 2.26tonnes and an effective natural period of 0.05sec (up to a displacement of 0.15m) as already illustrated in Figure 13. This same capacity curve is shown again in Figure 15 (but to a different scale).

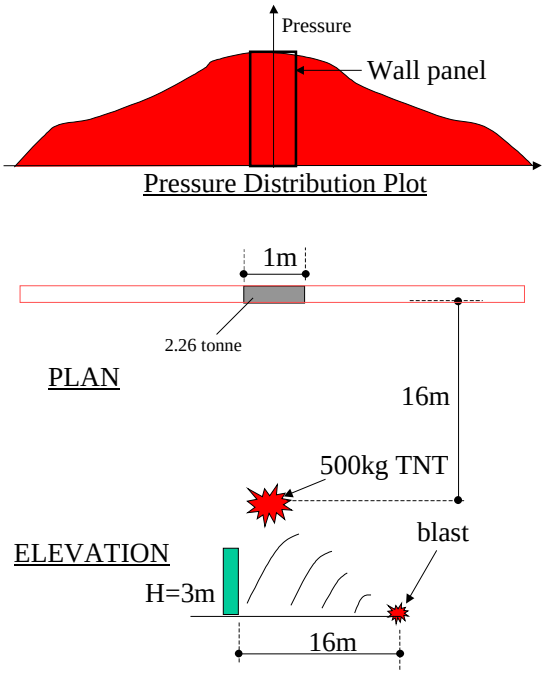

Figure 14: Example for Illustration

The scaled distance $\boldsymbol{Z}$ is calculated by $\dfrac{\boldsymbol{R}}{\boldsymbol{W}^{1/3}} = \dfrac{12}{500^{1/3}} = 1.5$ (from Eq.1)

The maximum over-pressure $\boldsymbol{Ps_{max}}$ is *5.4*bars(*540*kPa) (Figure 1 value x 1.8)

The coefficient of the reflected over-pressure $\boldsymbol{C_r}$ *=4.6* (from Eq.6 and Figure 6)

Total over-pressure = $\boldsymbol{Ps_{max}}$.$\boldsymbol{C_r}$ *= 540(4.6)=2500*kPa

Total blast load=2500kN/m^2 x 1m x 3m= *7500*kN

The Peak Acceleration $\boldsymbol{PA}$~*3320*m/sec^2 (340g's)

$$\boldsymbol{U} = \sqrt{\frac{6(5.4)+7}{7}}.(335) = 795\boldsymbol{m}/\sec$$ (from Eq.7b)

Clearing time $\boldsymbol{T'}$= $\dfrac{3(3\boldsymbol{m})}{795}$ =0.011sec (from Eq.7a)

$\dfrac{\boldsymbol{T}_1}{\boldsymbol{T}'} = 2.75$ (from Eq.11)

$\boldsymbol{T_1}$= 2.75(0.011)=0.03sec

$$\boldsymbol{RSV}_{\max} = 3320\left(\frac{0.03}{2\pi}\right) = 15.9\boldsymbol{m}/\sec$$ (from Eq.10b)

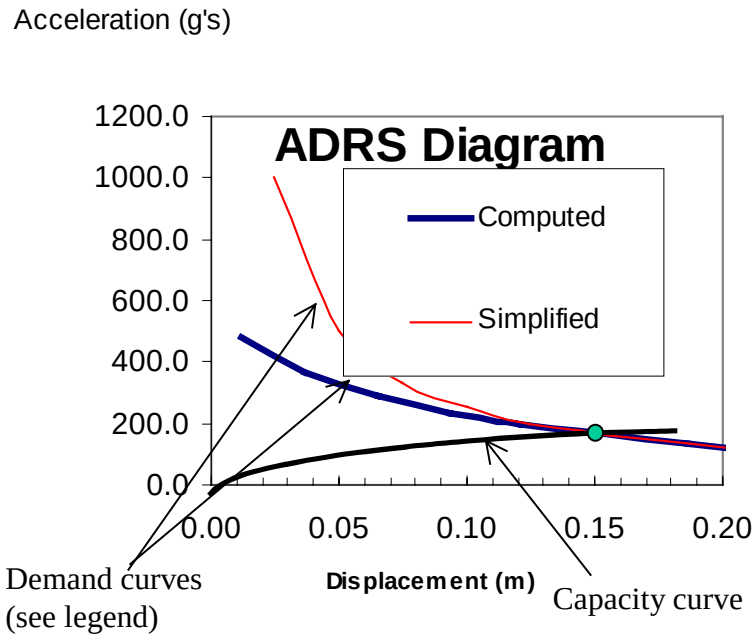

Figure 15: Capacity Spectrum and Performance Point Determination

The Demand curve in the ADRS format as defined by Eq.13 (with RSV_{max}=15.9m/sec) is plotted in Figure 15 as the "simplified" curve (see legend). The Capacity curve shown in the same figure was obtained from push-over analysis of the wall. The performance point was found to be at approximately 150mm (at the effective height) based on the interception of the Demand curve with the Capacity curve. The percentage drift of the wall when subject to the blast load is 5% (0.15/3=0.05).

7 Closing Remarks

Existing knowledge on the modelling of blast pressure have been further developed and applied in this paper for engineering applications. Parametric studies involving time-history analyses of simple wall models have been undertaken based on pre-defined pressure functions to study basic behaviour trends. The "corner period" (T_1) was found to be the key controlling parameter in the response spectrum modelling. An important contribution from this study is the identification of the direct relationship between T_1 and the "clearing time" (T') for the blast. A simple and realistic capacity spectrum model has been developed for the design and assessment of walls in withstanding blast loading. The practicality of the proposed model has been demonstrated herein by a worked example.

8 Acknowledgements

The authors are indebted to Dr Peter Smith of the Royal Military College of Science, United Kingdom who has given invaluable directions and advice to the authors during his recent visit to the University of Melbourne.

9 References

1. ATC-40. Seismic evaluation and retrofit of concrete buildings, Vols.1&2. Redwood City, CA: Applied Technology Council, 1996.
2. Brode HL "Numerical solution of spherical blast waves", *Journal of Applied Physics*, June 1955, No.6.
3. Chandler AM, Lam NTK, Wilson JL and Hutchinson GL. Review of Modern Concepts in the Engineering Interpretation of Earthquake Response Spectra, *ICE Proceedings : Structures and Buildings*. 146(10),75-84.
4. Nelson Lam, John Wilson. Displacement Modelling of Intraplate Earthquakes, International Seismology and Earthquake Technology Journal (special issue on Performance Based Seismic Design), 2004. Indian Institute of Technology. Accepted for publication and in-press.
5. Henrych J *The Dynamics of Explosion and its use* Elsevier Science Publisher, 1979.
6. Kingery CN and Bulmash G "Airblast parameters from TNT Spherical Air Blast and Hemispherical Surface Blast", *Technical Report ARBRL-TR-02555*. US Armament Research and Development Centre, Ballistic Research Laboratory, Aberdeen Proving Ground, MD, April 1984.
7. Smith PD and Hetherington JG *Blast and Ballistic Loading of Structures* , Butterowrth-Heinemann, Oxford 1994.

